- SUPPORTING INFORMATION -

Hafnium, titanium, and zirconium intercalation in 2D layered nanomaterials

*Vicky Huynh,[1,†] Kevin Rodriguez Rivera,[1,†] Tiffany Teoh,[1] Ethan Chen,[1] Jared Ura,[1] and Kristie J. Koski[1]**

[1] Department of Chemistry, University of California Davis, Davis California 95616, USA

*koski@ucdavis.edu

[†] These authors contributed equally

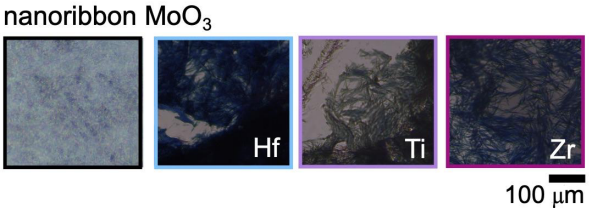

Figure S1. Optical images of hydrothermally grown nanoribbon MoO_3 deposited on a fused silica substrate and intercalated with Hf, Ti, and Zr showing color change from white to blue.

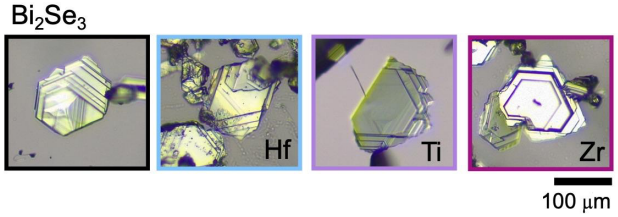

Figure S2. Optical images representative of Bi_2Se_3 intercalated with Hf, Ti, and Zr. Hf-intercalated Bi_2Se_3 shows a yellow hue. Zr-intercalated Bi_2Se_3 is somewhat more optically reflective.

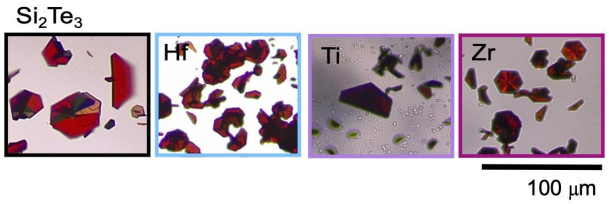

Figure S3. Optical images of Si_2Te_3 intercalated with Hf, Ti, and Zr. No obvious color change is observed.

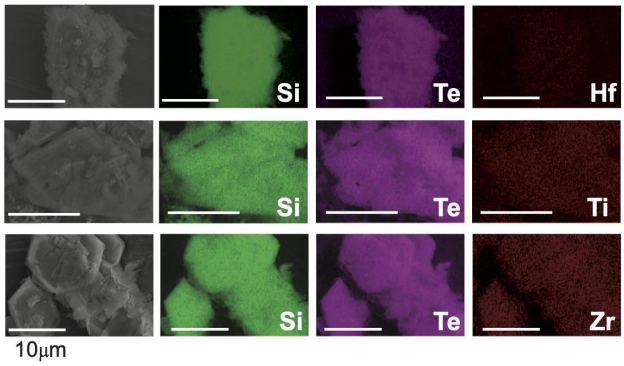

Figure S4. SEM-EDX map of Si_2Te_3 intercalated with Hf, Ti, Zr. The metals Hf, Ti, and Zr are detected throughout the crystals. Si_2Te_3 is air-sensitive. The mottled surfaces are due to hydrolysis and destruction of the Si_2Te_3 with exposure to air before placement into the SEM for measurement. Scalebars are 10 microns.

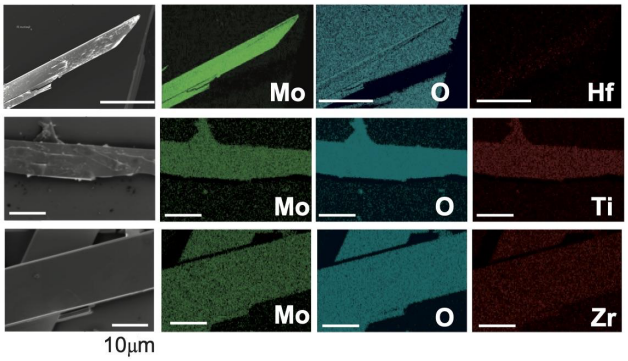

Figure S5. SEM-EDX map of MoO_3 intercalated with Hf, Ti, Zr. Hf-MoO_3 is on an oxide substrate so oxygen is detected everywhere. Hf, Ti, and Zr are found throughout the crystal. Scalebars are 10 μm.

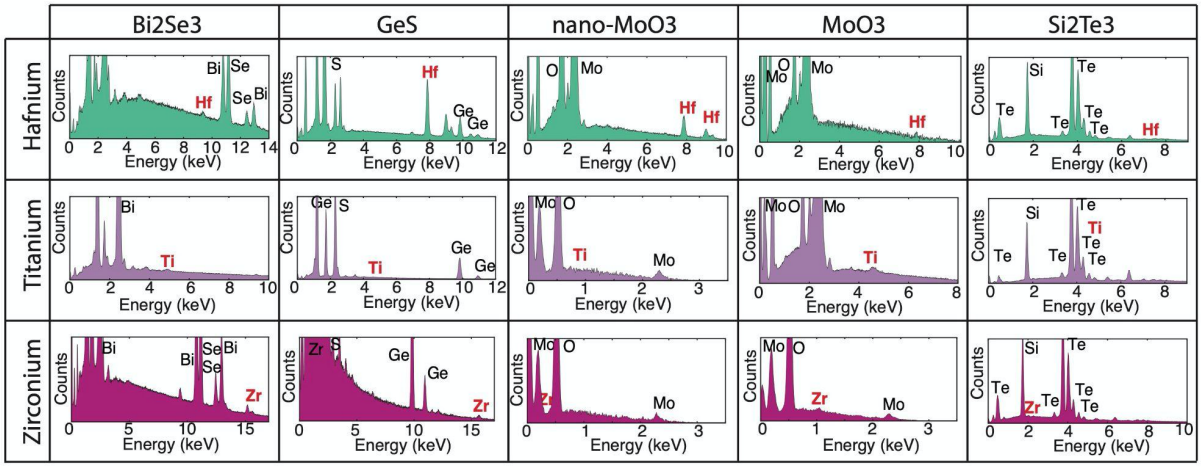

Figure S6. Table of SEM-EDX spectra of Bi_2Se_3, GeS, hydrothermally grown nanoribbon MoO_3, laterally large 2D MoO_3, and Si_2Te_3 intercalated with Hf, Ti, Zr.

	Hf max	Hf avg	Ti max	Ti avg	Zr max	Zr avg
Bi_2Se_3	0.26	0.03 ± 0.07	0.65	0.25 ± 0.21	6.4	1.40 ± 1.88
MoO_3	0.4	0.14 ± 0.14	8.5	2.97 ± 2.74	1.7	0.49 ± 0.56
nano-MoO_3	0.72	0.29 ± 0.27	6.71	2.00 ± 2.69	2.7	1.78 ± 0.65
GeS	3.6	0.76 ± 1.09	12.86	1.48 ± 4.28	2.8	1.24 ± 1.37
Si_2Te_3	1.2	1.03 ± 0.13	2.59	2.15 ± 0.24	0.41	0.18 ± 0.21

Table S1: Maximum and average atm % concentration of hafnium, titanium, or zirconium by SEM-EDX. Averages are made across 3-6 nanocrystals. There is large sample-to-sample variation which yields deviation in errors. Errors are calculated as the deviation across amounts detected in different crystals. nano- is hydrothermally grown MoO_3.

	a [Å]	c [Å]
Bi_2Se_3	4.145 ± 0.001	28.66 ± 0.01
Hf-Bi_2Se_3	4.147 ± 0.001	28.65 ± 0.01
Ti-Bi_2Se_3	4.144 ± 0.001	28.66 ± 0.01
Zr-Bi_2Se_3	4.144 ± 0.001	28.66 ± 0.01

Table S2. Lattice constants for intercalated Bi_2Se_3 nanoribbons determined through Le Bail fit of XRD patterns using GSAS-II.[1]

	b [Å]	b(2) [Å]
MoO_3	13.847 ± 0.007	—
Hf-MoO_3	13.854 ± 0.001	13.844 ± 0.001
Ti-MoO_3	13.854 ± 0.001	14.069 ± 0.069
Zr-MoO_3	13.844 ± 0.001	13.873 ± 0.001

Table S3. MoO_3 only shows one reflection (0k0). Lattice constants for intercalated MoO_3 ribbons determined through analysis of the peaks position and Rietveld refinement of XRD patterns using Maud.[2] The (0k0) peak splits in the Hf and Ti XRD pattern, so there are two different environments of MoO_3. Both sets of lattice parameters are presented.

	b [Å]
nano-MoO_3	13.830 ± 0.001
Hf-MoO_3	14.010 ± 0.005
Ti-MoO_3	14.01 ± 0.06
Zr-MoO_3	13.998 ± 0.001

Table S4. MoO_3 only shows one reflection (0k0). Lattice constants for hydrothermally grown MoO_3 nanoribbons determined through analysis of the peaks position and Rietveld refinement of XRD patterns using Maud.[2]

	a [Å]	b [Å]	c [Å]
GeS	4.301± 0.001	10.480 ± 0.001	3.644 ± 0.003
Hf-GeS	4.301 ± 0.001	10.480 ± 0.001	3.643 ± 0.003
Ti-GeS	4.302 ± 0.001	10.481 ± 0.001	3.644 ± 0.003
Zr-GeS	4.300 ± 0.001	10.477 ± 0.001	3.643 ± 0.003

Table S5. Lattice constants for all intercalated GeS platelets determined through Le Bail fit of XRD patterns using GSAS-II.[1]

	a [Å]	c [Å]
Si_2Te_3	7.429 ± 0.001	13.478 ± 0.001
Hf-Si_2Te_3	7.429 ± 0.001	13.487 ± 0.001
Ti-Si_2Te_3	7.427 ± 0.001	13.482 ± 0.001
Zr-Si_2Te_3	7.422 ± 0.001	13.470 ± 0.001

Table S6. Lattice constants for all intercalated Si_2Te_3 nanoribbons determined through Le Bail fit of XRD patterns using GSAS-II.[1]

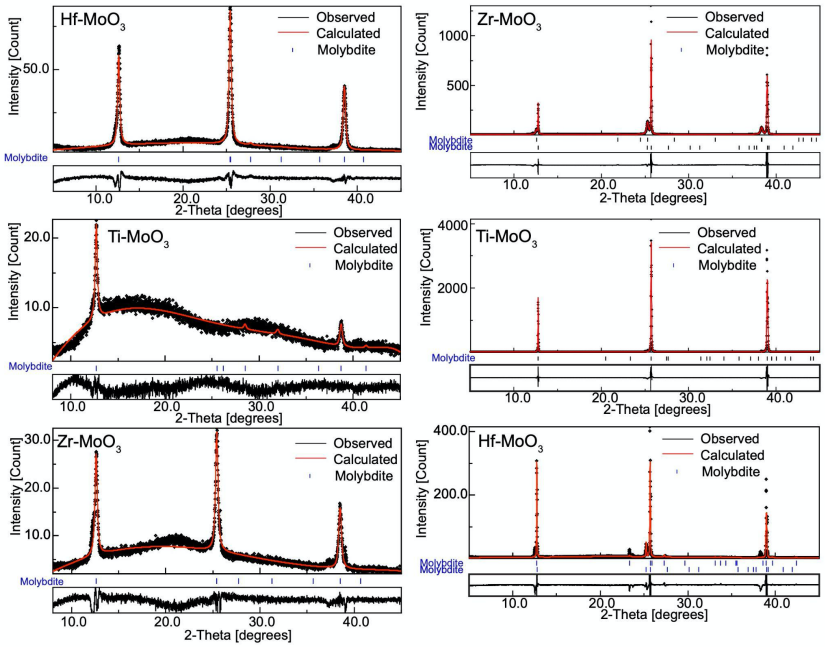

Figure S7. Rietveld Refinement of MoO_3 using Maud.[2] Only one reflection is measured.

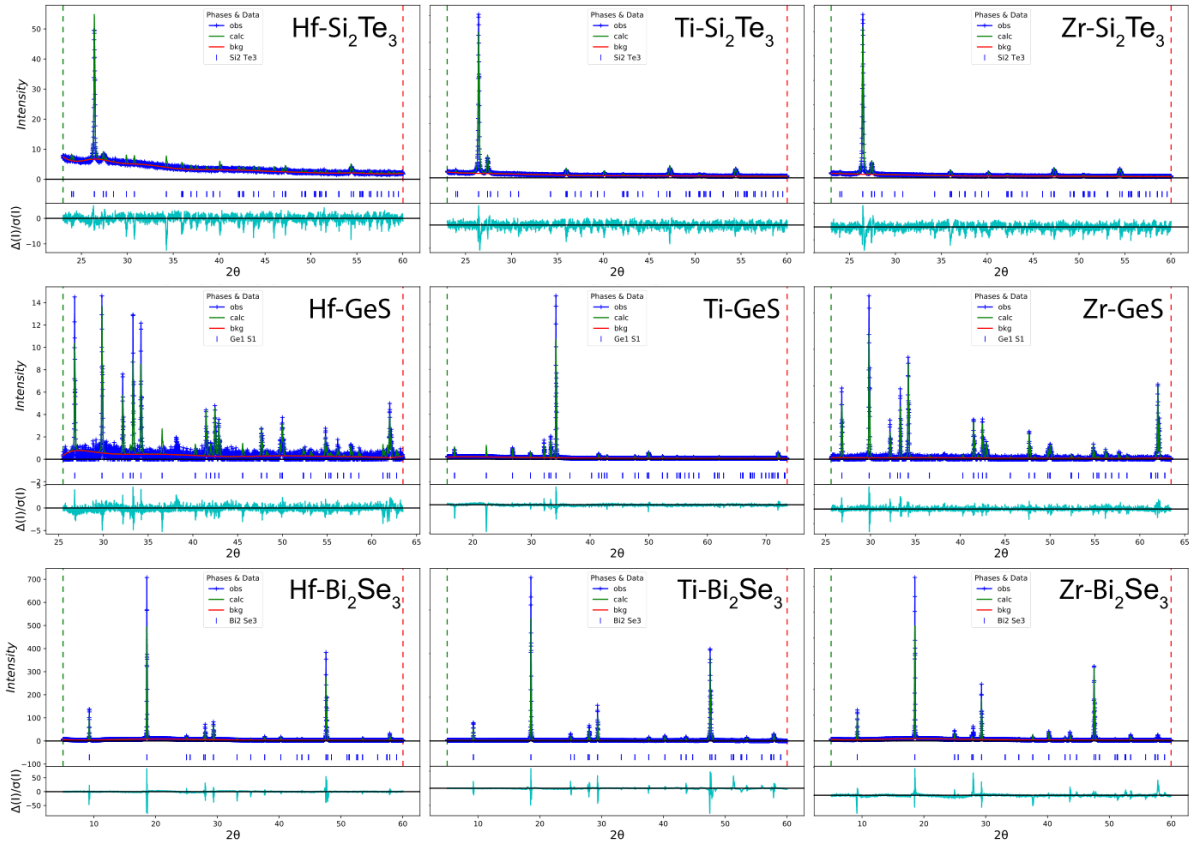

Figure S8. Le Bail fits of Si_2Te_3 (top), GeS (middle), Bi_2Se_3 (bottom) using GSAS-II.[1]

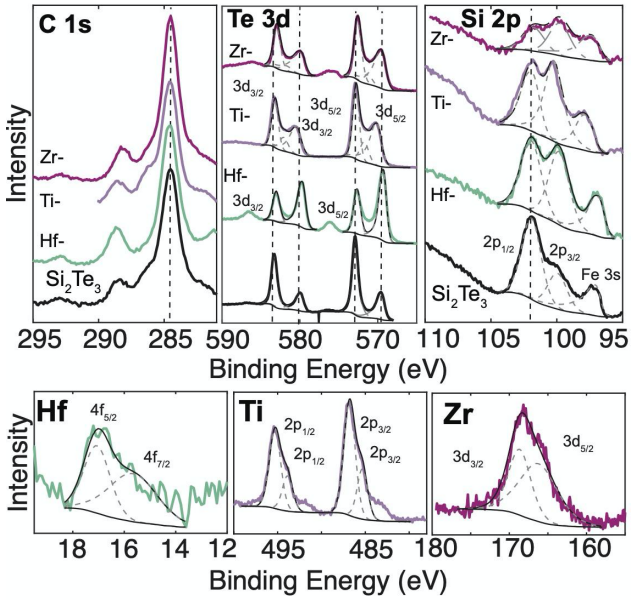

Figure S9. XPS spectra of Si_2Te_3 intercalated with Hf, Ti, and Zr. Adventitious carbon (284.5 eV) is used to calibrate charge across different samples. Si_2Te_3 is sensitive to oxygen exposure which affects XPS characterization. Si_2Te_3 shows a tellurium 3d doublet in all samples showing two distinct tellurium environments in Si_2Te_3. The Te doublet shifts to lower binding energies indicating an increase in electron density and charge transfer from the intercalant to the host. Hf-Si_2Te_3 shows a change in intensity in the tellurium doublets. The Si 2p does not shift much with intercalation. Si sits in Si-Si dumbbells in Si_2Te_3 and shows little electronic interaction with the intercalant. An Fe 3s peak is from the stainless steel substrate used to hold the Si_2Te_3 for characterization in the XPS.

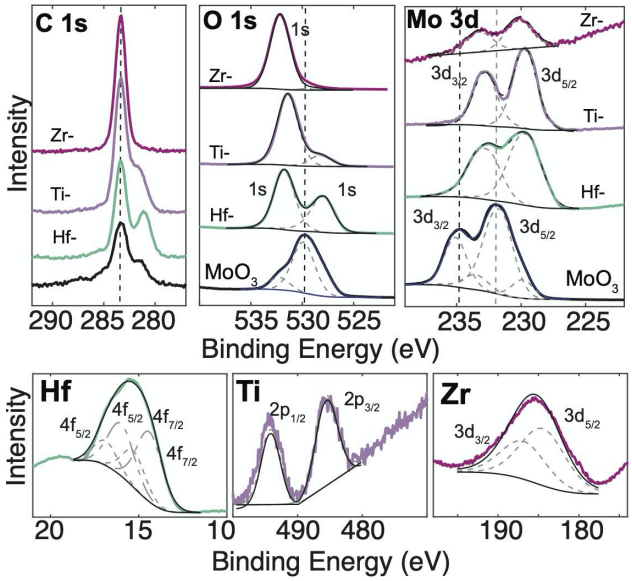

Figure S10. XPS of nanoribbon-MoO_3 grown through hydrothermal synthesis intercalated with Hf, Ti, and Zr. This MoO_3, by virtue of its growth, has additional liquid organic sources of carbon which obfuscates calibration with the adventitious carbon. The strongest peak is assumed to be the adventitious carbon, to calibrate charge across samples (284.5 eV). The O 1s binding energy increases in all samples. Hf-MoO_3 shows two 1s peaks which would indicate two different oxidation environments, which are reflected in the XRD diffraction patterns (Article; Figure 2) that show two different environments for Hf-intercalated MoO_3. The Mo 3d peak shows a decrease in the binding energy for all samples. These two competing effects are interesting. They suggest that the electrons on the oxygen are donated to the intercalant guest, except in the alternate Hf environment, while the Mo peaks show electrons are donated to the Mo and an increase in the screening of core electrons. Mo 3d behaves very differently in the hydrothermally and vapor phase grown MoO_3. The differences in Figure 9 and Figure S10 in these two differently grown MoO_3 samples with hydrothermally grown MoO_3 showing an increase in the screening of the Mo and vapor grown samples showing a decrease, may be attributed to the water remaining in the van der Waals gap from hydrothermal growth.

	Peak	B.E. (eV)	FWHM
Bi Bi_2Se_3	4f 7/2	158.14	0.85
	4f 5/2	163.43	0.89
Hf	4f 7/2	158.22	0.82
	4f 5/2	163.53	0.75
	4f 7/2	159.68	1.09
	4f 5/2	164.89	1.09
Ti	4f 7/2	157.54	0.79
	4f 5/2	162.85	0.79
Zr	4f 7/2	157.32	0.94
	4f 5/2	162.63	0.94

Table S7. Peak fits for Bi 4f in Hf, Ti, Zr-intercalated Bi_2Se_3 using ESCApe.

	Peak	B.E. (eV)	FWHM
Se Bi_2Se_3	3d 5/2	53.59	0.77
	3d 3/2	54.45	0.86
Hf	3d 5/2	53.61	0.82
	3d 3/2	54.47	0.76
Ti	3d 5/2	52.96	0.80
	3d 3/2	53.82	0.75
Zr	3d 5/2	52.87	0.97
	3d 3/2	53.73	0.88

Table S8. Peak fits for Se 3d in Hf, Ti, Zr-intercalated Bi_2Se_3.

	Peak	B.E. (eV)	FWHM
Ge GeS	3d	30.20	1.28
	3d	30.90	1.28
Hf	3d 5/2	29.80	0.63
	3d 3/2	30.37	0.69
	3d	31.78	1.40
	3d	32.85	1.40
Ti	3d	32.84	0.71
	3d	33.45	0.71
Zr	3d 5/2	32.19	1.26
	3d 5/2	30.24	1.21
	3d 3/2	31.22	1.21
	3d 3/2	33.02	1.26

Table S9. Peak fits for Ge 3d in Hf, Ti, Zr-intercalated GeS.

	Peak	B.E. (eV)	FWHM
S GeS	2p	164.39	0.96
	2p	165.53	0.84
Hf	2p3/2	161.29	0.87
	2p1/2	162.43	0.82
Ti	2p	164.23	0.79
	2p	165.44	0.78
Zr	2p3/2	161.60	1.31
	2p1/2	162.82	1.22

Table S10. Peak fits for S 2p in Hf, Ti, Zr-intercalated GeS.

	Peak	B.E. (eV)	FWHM
Mo MoO_3	3d 5/2	232.52	0.84
	3d 3/2	235.66	0.88
Hf	3d 5/2	232.98	1.22
	3d 3/2	236.11	1.25
	3d 5/2	231.44	1.18
	3d 3/2	234.57	1.05
Ti	3d 5/2	233.59	1.22
	3d 3/2	236.72	1.29
	3d 5/2	232.37	1.78
	3d 3/2	235.50	1.71
Zr	3d	232.63	0.91
	3d	235.76	0.96

Table S11. Peak fits for Mo 4f in Hf, Ti, Zr-intercalated MoO_3.

	Peak	B.E. (eV)	FWHM
O MoO_3	1s	530.30	1.10
	1s	531.89	1.10
Hf	1s	531.17	1.63
	1s	532.55	1.63
Ti	1s	530.48	1.59
	1s	531.81	1.59
Zr	1s	530.46	1.20
	1s	531.86	1.20

Table S12. Peak fits for O 4f in Hf, Ti, Zr-intercalated MoO_3.

	Peak	B.E. (eV)	FWHM
Mo nano-MoO_3	3d 5/2	230.14	2.45
	3d 3/2	233.27	2.45
Hf	3d 5/2	229.58	2.96
	3d 3/2	232.71	2.96
Ti	3d 5/2	229.66	2.15
	3d 3/2	232.79	2.15
Zr	3d	230.14	2.45
	3d	233.27	2.45

Table S13. Peak fits for Mo 4f in Hf, Ti, Zr-intercalated hydrothermally grown nanoribbon MoO_3.

	Peak	B.E. (eV)	FWHM
O nano-MoO_3	1s	528.87	2.28
	1s	532.14	2.28
Hf	1s	527.87	2.63
	1s	531.71	2.39
Ti	1s	528.23	2.40
	1s	531.44	2.40
Zr	1s	528.87	2.28
	1s	532.14	2.28

Table S14. Peak fits for O 4f in Hf, Ti, Zr-intercalated hydrothermally grown nanoribbon MoO_3.

	Peak	B.E. (eV)	FWHM
Si Si_2Te_3	2p	101.92	1.71
	2p	99.95	1.71
Hf	2p	99.83	1.82
	2p	101.95	1.82
Ti	2p	100.24	1.66
	2p	101.89	1.66
Zr	2p	99.78	1.88
	2p	101.76	1.88

Table S15. Peak fits for Si 4f in Hf, Ti, Zr-intercalated Si_2Te_3.

	Peak	B.E. (eV)	FWHM
Te Si_2Te_3	3d 5/2	572.88	0.91
	3d 3/2	583.27	0.84
	3d 5/2	569.53	1.27
	3d 3/2	579.88	1.35
Hf	3d 5/2	569.27	1.11
	3d 3/2	579.69	1.26
	3d 5/2	572.66	1.03
	3d 3/2	583.04	1.03
Ti	3d 5/2	572.79	0.98
	3d 3/2	583.19	0.98
	3d 5/2	570.06	1.75
	3d 3/2	580.36	1.75
	3d 3/2	582.08	1.28
	3d 5/2	571.73	1.28
Zr	3d 5/2	572.54	1.11
	3d 3/2	582.93	1.09
	3d 5/2	569.50	1.77
	3d 3/2	579.89	1.91
	3d 5/2	571.23	1.29
	3d 3/2	581.76	1.44

Table S16. Peak fits for Te 4f in Hf, Ti, Zr-intercalated Si_2Te_3.

Hf	Peak	B.E. (eV)	FWHM
Hf Bi_2Se_3	4f 7/2	16.80	1.85
	4f5/2	18.89	2.52
Hf GeS	4f 7/2	17.57	1.30
	4f5/2	19.24	1.26
Hf MoO_3	4f	17.25	1.40
	4f	18.96	1.49
Hf nano- MoO_3	4f 7/2	14.39	1.73
	4f5/2	15.99	1.73
	4f 7/2	15.28	1.56
	4f5/2	16.88	1.56
Si_2Te_3	4f 7/2	15.66	2.23
	4f5/2	17.06	1.19

Table S17. Peak fits for Hf 4f in Hf-intercalated Bi_2Se_3, GeS, MoO_3 , hydrothermally grown MoO_3, and Si_2Te_3.

Ti	Peak	B.E. (eV)	FWHM
Ti Bi_2Se_3	2p	458.47	3.58
	2p	464.01	3.58
Ti GeS	2p	461.88	1.74
	2p	467.42	3.52
Ti MoO_3	2p1/2	459.52	2.62
	2p3/2	465.06	2.20
Ti nano- MoO_3	2p1/2	494.11	3.56
	2p3/2	485.47	4.16
Si_2Te_3	2p1/2	486.80	1.52
	2p3/2	495.30	1.52
	2p1/2	485.34	1.40
	2p3/2	493.87	1.40

Table S18. Peak fits for Ti 2p in Ti-intercalated Bi_2Se_3, GeS, MoO_3, hydrothermally grown MoO_3, and Si_2Te_3.

Zr	Peak	B.E. (eV)	FWHM
Zr Bi_2Se_3	3d	182.30	1.48
	3d	184.67	1.97
Zr GeS	3d5/2	182.66	1.60
	3d3/2	185.00	1.47
Zr MoO_3	3d	182.60	1.23
	3d	185.00	1.22
Zr nano-MoO_3	3d5/2	184.42	6.57
	3d3/2	186.85	6.57
Si_2Te_3	3d3/2	168.65	3.40
	3d5/2	166.22	5.80

Table S19. Peak fits for Zr 3d in Zr-intercalated Bi_2Se_3, GeS, MoO_3, hydrothermally grown MoO_3, and Si_2Te_3.

REFERENCES

(1) Toby, B.H. and Von Dreele, R.B., GSAS-II: the genesis of a modern open-source all purpose crystallography software package. *J. Appl. Crystallogr,* **2013**, *46*, 544-549.

(2) Lutterotti, L.; Matthies, S.; and Wenk, H. MAUD: a friendly Java program for material analysis using diffraction. IUCr: *Newsletter of the CPD* **1999**, 21.